This article was downloaded by:
On: *14 January 2011*
Access details: *Access Details: Free Access*
Publisher *Taylor & Francis*
Informa Ltd Registered in England and Wales Registered Number: 1072954 Registered office: Mortimer House, 37-41 Mortimer Street, London W1T 3JH, UK

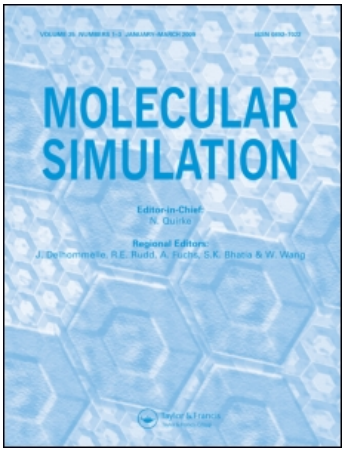

Molecular Simulation
Publication details, including instructions for authors and subscription information:
http://www.informaworld.com/smpp/title~content=t713644482

On the Choice of Dihedral Angle Potential Energy Functions for *n*-Alkanes

Lukas D. Schuler[a]; Wilfred F. Van Gunsteren[a]
[a] Department of Physical Chemistry, Swiss Federal Institute of Technology Zürich, Zürich, Switzerland

To cite this Article Schuler, Lukas D. and Van Gunsteren, Wilfred F.(2000) 'On the Choice of Dihedral Angle Potential Energy Functions for *n*-Alkanes', Molecular Simulation, 25: 5, 301 — 319
To link to this Article: DOI: 10.1080/08927020008024504
URL: http://dx.doi.org/10.1080/08927020008024504

PLEASE SCROLL DOWN FOR ARTICLE

Full terms and conditions of use: http://www.informaworld.com/terms-and-conditions-of-access.pdf

This article may be used for research, teaching and private study purposes. Any substantial or systematic reproduction, re-distribution, re-selling, loan or sub-licensing, systematic supply or distribution in any form to anyone is expressly forbidden.

The publisher does not give any warranty express or implied or make any representation that the contents will be complete or accurate or up to date. The accuracy of any instructions, formulae and drug doses should be independently verified with primary sources. The publisher shall not be liable for any loss, actions, claims, proceedings, demand or costs or damages whatsoever or howsoever caused arising directly or indirectly in connection with or arising out of the use of this material.

Molecular Simulation, 2000, Vol. 25, pp. 301–319
Reprints available directly from the publisher
Photocopying permitted by license only

© 2000 OPA (Overseas Publishers Association) N.V.
Published by license under
the Gordon and Breach Science
Publishers imprint.
Printed in Malaysia.

ON THE CHOICE OF DIHEDRAL ANGLE POTENTIAL ENERGY FUNCTIONS FOR *n*-ALKANES

LUKAS D. SCHULER and WILFRED F. VAN GUNSTEREN*

Department of Physical Chemistry, Swiss Federal Institute of Technology Zürich, ETH-Zentrum, 8092 Zürich, Switzerland

(Received November 1999; accepted November 1999)

Downloaded At: 18:55 14 January 2011

The parameters of the GROMOS96 force field governing dihedral angle transitions in aliphatic chains have been reconsidered, since these parameters produce a too large ratio of *trans* to *gauche* conformations in such chains. A refined set of parameters for dihedral angle interactions and third-neighbour interactions involving CH_2 and CH_3 atoms is proposed. They were obtained by fitting to the heat of vaporization, pressure and *trans-gauche* ratio for liquids of three *n*-alkanes, *n*-butane, *n*-pentane and *n*-hexane. The new parameter set does reproduce better these quantities and should therefore be more appropriate for use in simulations of polymers and membranes. A comparison of the mentioned properties obtained from simulations with united-atom models and from simulations with an all-atom model shows that the latter does not necessarily yield an improved description of molecular behaviour.

Keywords: *n*-Alkanes; force field parameters; GROMOS force field; molecular dynamics simulation; *trans-gauche* energy differences

1. INTRODUCTION

The practical value of computer simulation of molecular systems relies very much on the accuracy of the potential energy function or force field that is used. For biomolecular systems a number of force fields have been developed and refined during the past decades, and are widely used [1–13, 50]. The potential energy functions of different force fields have slightly different forms, and the force field parameters are generally obtained by fitting of a range of molecular properties against different sets of quantum-mechanical

*Corresponding author.

and experimental data regarding small molecules. A force field can be tested by application to biomolecular systems for which structural, energetic and dynamic data are available.

When using the most recent version of the GROMOS (Groningen Molecular Simulation) force field [11, 14, 15] in simulations of membranes, which involve – in contrast to proteins, sugars and nucleotides – long aliphatic carbon chains, we observed that the GROMOS96 43A1 force field [11] favours too strongly *trans* over *gauche* conformations in aliphatic chains. In the parametrisation of the GROMOS 43A1 force field, the CH_1, CH_2 and CH_3 united-atom van der Waals interaction parameters had been determined such that the energy (heat of vaporization) and density of a number of *n*-alkanes in the liquid phase was reproduced [14]. The parameters of the torsional angle term in the force field had not been changed from the previous force field version [16]. Thus, these could be varied to obtain values for which a correct *trans-gauche* ratio is obtained, while still maintaining the correct energy and density of the *n*-alkane liquids.

We report a refinement of the parameters for aliphatic chains in the GROMOS 43A1 force field. The experimental and quantum-mechanically calculated data used in the parametrisation are considered, and a comparison of the properties of the *n*-alkanes butane, pentane and hexane obtained using various parameter sets and also using OPLS parameters [12, 13] is presented. The effects of using different cut-off radii for the intermolecular non-bonded interactions is considered in an appendix.

Downloaded At: 18:55 14 January 2011

2. SELECTION OF TARGET VALUES FOR THE PARAMETRISATION

First, the target values to be used in the parametrisation have to be chosen. As target values for the heat of vaporization ΔH_{vap} and the pressure p (for a given density) for *n*-butane, *n*-pentane and *n*-hexane were taken experimental values for these quantities [17], as in [14]. To select a target value for the ratio of *trans* to *gauche* conformations or for the *gauche-trans* energy difference, values obtained by spectroscopic measurements or by quantum-theoretical model calculations were considered. Over several decades, a range of experimental and theoretical values has been published, as is illustrated for *n*-butane in Figure 1. The most recent data seem to converge around $2.7\,kJ \cdot mol^{-1}$. We have chosen the average of the encircled data points as target value for the *n*-butane *gauche-trans* energy difference: $2.66 \pm 0.16\,kJ \cdot mol^{-1}$. A similar procedure was followed to select the target *gauche-trans* difference $E_g - E_t$ for *n*-pentane and *n*-hexane, see Table I.

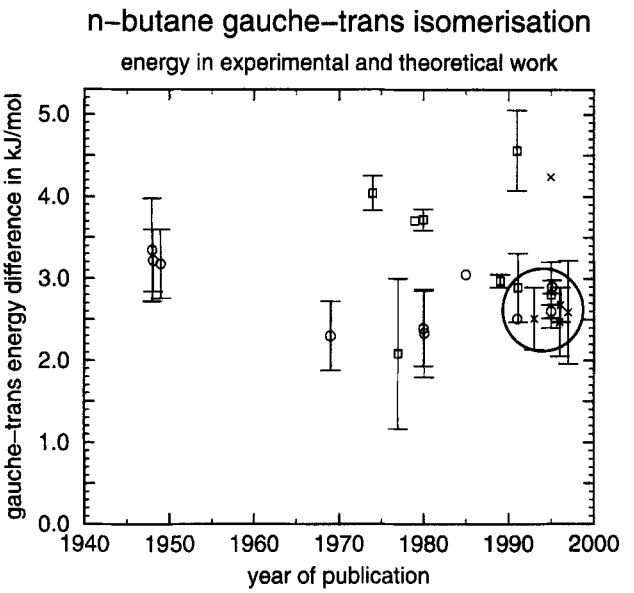

FIGURE 1 Over several decades, *n*-butane *gauche-trans* energy difference was measured in the liquid phase (circles), gas phase (squares) and calculated by high-level *ab initio* methods (crosses). Error bars are shown whenever the data was available. The average of the encircled data was chosen as target value for the aliphatic GROMOS force field parameters. It amounts to 2.66 ± 0.16 kJ/mol. References for the data and experimental methods are found in [18] to [36].

TABLE I Target value determination for energy differences between different conformations of *n*-alkanes. The relative potential energies E are indicated through their differences by letters g for the *gauche* and t for the *trans* conformation and both letters for the barriers between the two conformations. The sources of data are shown by reference number. If more than one reference is given, the average was taken even if different methods or molecules of similar dihedral properties were involved. In the case of *n*-pentane some low-level *ab-initio* calculations have been made (result section, Fig. 2)

Molecule	E_{pot}	*References*	*Target value [kJ/mol]*
n-Butane	$E_g - E_t$	[29, 31, 32, 33, 35, 36]	2.66 ± 0.16*
	$E_{tg} - E_t$	[35]	13.85 ± 0.42¶
	$E_{gg} - E_t$	[35]	22.93 ± 2.09¶
n-Pentane	$E_g - E_t$	[19, 24, 29, 32, 37, 38, 39, 40]	2.26 ± 0.25§
	$E_{tg} - E_t$	–	–
	$E_{gg} - E_t$	–	–
n-Hexane	$E_g - E_t$	[35, 41]	2.14 ± 0.16#
	$E_{tg} - E_t$	[35]	11.76 ± 0.42¶
	$E_{gg} - E_t$	[35]	21.67 ± 0.42¶

* average over several methods,
¶ best available *ab-initio* level result,
§ average over all data and
# average over larger molecules.

Downloaded At: 18:55 14 January 2011

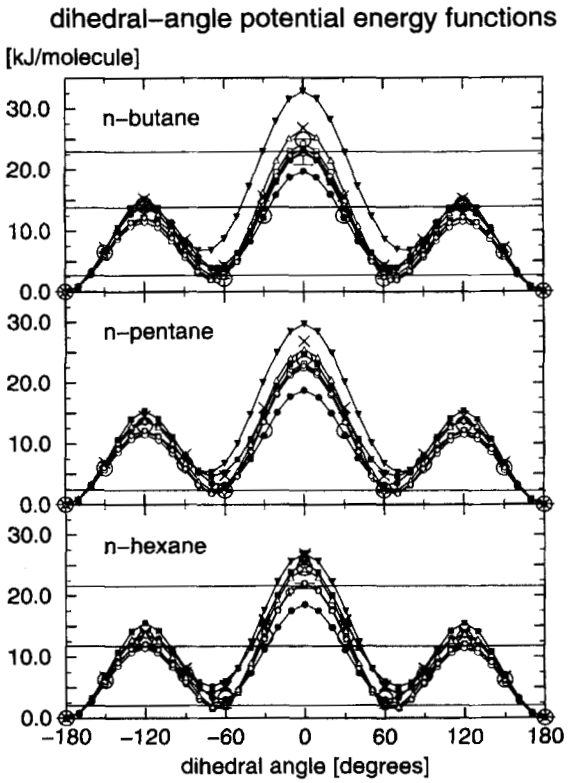

FIGURE 2 The original GROMOS96 potential energy as function of dihedral angle value for *n*-butane, *n*-pentane and *n*-hexane is shown as eyeguiding line with filled triangles. Target energy values derived from experimental or theoretical work (Tab. I) are indicated with horizontal lines.

The modifications of the GROMOS96 force field, in which the third-neighbour van der Waals repulsive (CS_{12}) parameter was reduced and the force constant (K_{φ_n}) for alkane dihedral angle potentials was increased (Tab. II), are shown as eyeguiding lines with open white triangles (a), squares (b), circles (c) or diamonds (d).

The result for the OPLS united- and all-atom force fields were obtained using a modified version of the GROMOS96 software (for all-atom electrostatic 1–4 scaling). The results are shown as filled circles (united-atom) or filled squares (all-atom) including an eyeguiding line.

Additional values illustrated are: Hartree Fock for several basis sets (up to 6–31G**, large crosses) and MP2 6–31G** (large circles).

Literature values from high-level *ab-initio* quantum calculations were used to obtain target values for the energy difference $E_{tg} - E_t$ between the *trans/gauche* barrier and the *trans* conformation, and for the energy difference $E_{gg} - E_t$ between the *gauche/gauche* or *cis* barrier and the *trans* conformation, see Table I.

Downloaded At: 18:55 14 January 2011

3. MODEL CALCULATIONS AND SIMULATIONS

The functional form of the GROMOS96 force field has been given in Refs. [11, 14, 15, 42]. The terms representing torsional interactions and non-bonded interactions are

$$V^{\text{trig}}(\vec{r}) = \sum_{n=1}^{N_\varphi} K_{\varphi_n}\left[1 + \cos(\delta_n)\cos(m_n\varphi_n(\vec{r}))\right] \tag{1}$$

and

$$V^{\text{nonb}}(\vec{r}) = \sum_{\substack{\text{non-bonded}\\ \text{pairs } (i,j)}} \left[\frac{C_{12}(i,j)}{r_{ij}^6} - C_6(i,j)\right]\frac{1}{r_{ij}^6} + \sum_{\substack{\text{non-bonded}\\ \text{pairs } (i,j)}} \frac{q_i q_j}{4\pi\varepsilon_0\varepsilon_1}\left[\frac{1}{r_{ij}} - \frac{C_{rf}r_{ij}^2}{2R_{rf}^3} - \frac{1-(1/2)C_{rf}}{R_{rf}}\right] \tag{2}$$

The summation in (1) runs over the N_φ dihedral or torsional angles $\varphi_n(\vec{r})$ in the molecules, which depend on the Cartesian coordinates $\vec{r}$ of the atoms in the system. The parameters of the torsional interaction term for dihedral angle φ_n are the force constant K_{φ_n}, phase shift δ_n and multiplicity m_n. The summation over the non-bonded pairs (i,j) requires some clarification. No non-bonded interaction is calculated for atom pairs that are connected by one or two bonds (or in special cases not considered here, three bonds) and slightly weaker van der Waals interactions are used for certain atom types, *e.g.*, the aliphatic CH_1, CH_2 and CH_3 united atoms considered here, separated by three bonds. These are called third-neighbour or 1–4 van der Waals interactions and parameters ($CS_{12}(i,j)$ and $CS_6(i,j)$ replacing $C_{12}(i,j)$ and $C_6(i,j)$ in (2)). The distance between atoms i and j is indicated by r_{ij}. The second term in (2), Coulomb plus reaction field, only applies when the atoms carry non-zero partial charges q_i. For aliphatic carbons in the GROMOS and OPLS *united-atom* force fields these charges are zero. In the calculations using the OPLS all-atom force field, we used a dielectric permittivity of 1 ($\varepsilon_1 = \varepsilon_2 = 1.0$) both inside ($\varepsilon_1$) and outside ($\varepsilon_2$) the long-range cut-off radius $R_{rf} = 1.4$ nm. Since the ionic strength of the *n*-alkane liquids is zero, the inverse Debye screening length κ is also zero, which means that $C_{rf} = 0$ in (2).

In the GROMOS force field, the general van der Waals parameters $C_{12}(i,j)$ and $C_6(i,j)$ and the third-neighbour van der Waals parameters

Downloaded At: 18:55 14 January 2011

$CS_{12}(i,j)$ and $CS_6(i,j)$ are defined separately for each pair of atom types. It is possible within the GROMOS force field to parametrise self-interactions (between pairs of identical atoms) separately from crossed interactions (between different atom types). The force field doesn't depend on a given set of combination rules, which adds considerable flexibility to the parametrisation. By default, however, the parameters for crossed interactions are generated by taking the geometric mean of the self-interaction values: $C_{12}(i,j) = [C_{12}(i,i) \cdot C_{12}(j,j)]^{1/2}$ and $C_6(i,j) = [C_6(i,i) \cdot C_6(j,j)]^{1/2}$, and likewise for the third-neighbour van der Waals parameters $CS_{12}(i,j)$ and $CS_6(i,j)$. Improvement of the *trans-gauche* ratio for aliphatic carbon chains or *n*-alkanes only involves a refitting of the torsional angle interaction parameter K_{φ_n} for dihedrals of type $\square\text{—}CH_n\text{—}CH_n\text{—}\square$ and of the third-neighbour van der Waals parameters $CS_{12}(CH_2, CH_2)$, CS_{12} (CH_3, CH_3), $CS_6(CH_2, CH_2)$ and $CS_6(CH_3, CH_3)$. It turned out that the latter two parameters could be kept at their GROMOS96 43A1 values while varying the other three parameters to fit the calculated liquid energy, pressure and *trans-gauche* ratio for the three *n*-alkanes to the target values given in Table II.

The GROMOS96 software [11] was used in all simulations. For the investigation of liquid alkane properties, 512 molecules ($= N_{\text{molecule}}$) have been used within a cubic box under periodic boundary conditions. The box length l_{box} chosen corresponds to the experimental density at 298.15 K of the liquid (ρ_{liquid}) and is calculated through Eq. (3) leading to 4.41814 nm for *n*-butane, 4.62264 nm for *n*-pentane and 4.80535 nm for *n*-hexane.

$$l_{\text{box}} = \left(\frac{N_{\text{molecule}} \cdot M_{\text{molecule}}}{\rho_{\text{liquid}}} \right)^{1/3}, \tag{3}$$

where M_{molecule} is the mass of an *n*-alkane molecule. Starting from a regular array of molecules, a molecular dynamics simulation at constant volume and temperature (NVT) of 500 ps was carried out. Initial velocities were taken from a Maxwellian distribution at 298.15 K and the initial centre of mass motion was removed. The time coupling constant for coupling to the temperature bath was set to $\tau_T = 0.1$ ps [44]. The time step used in the leap-frog integration scheme was 0.002 ps. Except for bond constraints maintained at a relative geometrical tolerance of 10^{-4} by the SHAKE algorithm [45] all internal interactions were treated explicitly. A twin range cutoff of 0.8/1.4 nm was applied to the non-bonded interactions and the non-bonded pairlist and the long-range forces were updated every 5 time steps.

Downloaded At: 18:55 14 January 2011

Downloaded At: 18:55 14 January 2011

TABLE II Comparison of properties for different combinations of force field parameters. GROMOS96 third-neighbour non-bonded and dihedral angle potential parameters were tested using *n*-alkane simulations. New parameter sets (a to d) were used to improve the dihedral angle potential energy profiles (Fig. 2). Results have been compared to OPLS united-atom and all-atom approaches. Reference values for experimental heat of vaporization and pressure are found in [17], those for the percentages of *trans* configuration are interpolated from [24, 29, 31, 43] for *n*-butane, from [24, 29] for *n*-pentane and from [29] for *n*-hexane, where the value in parentheses is an average measured for longer *n*-alkanes also from [29]

Forcefield	*Parameters*					*Properties*			
Name, interaction	*Dihedral potential*			*1–4 van der Waals parameters*		ΔH_{vap}	*p*	r_{geom}	*Number of transitions*
n-Butane, CH_3—CH_3	K_{φ_n}	δ_n	m_n	$CS_{12}(CH_3, CH_3)$	$CS_6(CH_3, CH_3)$	[*kJ/mol*]	[*atm*]	[%]	[*per dihedral per 100 ps*]
Experimental target						**21.62**	**2.43**	**60**	–
GROMOS96 43A1	5.86	+1	3	0.1206173E-04	0.6852528E-02	20.76	130.13	91	1.72
GROMOS96a	7.08	+1	3	0.6793766E-05	0.6852528E-02	20.87	124.87	66	1.79
GROMOS96b	6.28	+1	3	0.6412316E-05	0.6852528E-02	20.74	121.64	63	3.08
GROMOS96c 43A2	5.92	+1	3	0.6030865E-05	0.6852528E-02	21.00	121.77	60	3.79
GROMOS96d	6.28	+1	3	0.6030865E-05	0.6852528E-02	20.84	108.80	59	3.00
OPLS ua	3.18402	+1	1	0.0	0.0	21.05	130.11	68	2.56
	−0.65898	−1	2						
	6.70904	+1	3						
OPLS aa	3.640080	+1	1	0.1866303E-05	0.1015252E-02	21.20	131.27	74	2.00
	−0.328444	−1	2						
	0.583668	+1	3						
n-Pentane, CH_3—CH_2	K_{φ_n}	δ_n	m_n	$CS_{12}(CH_2, CH_3)$	$CS_6(CH_2, CH_3)$	[*kJ/mol*]	[*atm*]	[%]	[*per dihedral per 100 ps*]
Experimental target						**26.43**	**0.68**	**64**	–
GROMOS96 43A1	5.86	+1	3	0.9262491E-05	0.5689469E-02	26.30	40.92	86	2.41, 2.42
GROMOS96a	7.08	+1	3	0.5675873E-05	0.5689469E-02	26.12	31.39	69	1.92, 2.03
GROMOS96b	6.28	+1	3	0.5347702E-05	0.5689469E-02	26.47	35.76	66	3.15, 3.10
GROMOS96c 43A2	5.92	+1	3	0.5347702E-05	0.5689469E-02	26.09	24.64	66	3.74, 3.84
GROMOS96d	6.28	+1	3	0.5186203E-05	0.5689469E-02	25.96	25.93	65	3.11, 3.16
OPLS ua	2.95181	+1	1	0.0	0.0	26.25	39.90	72	2.71, 2.72
	−0.56693	−1	2						
	6.57934	+1	3						
OPLS aa	3.640080	+1	1	0.1866303E-05	0.1015252E-02	26.37	117.74	80	1.64, 1.64
	−0.328444	−1	2						
	0.583668	+1	3						

Downloaded At: 18:55 14 January 2011

TABLE II (Continued)

Forcefield	*Parameters*					*Properties*			
Name, interaction	*Dihedral potential*			*1–4 van der Waals parameters*		ΔH_{vap}	p	r_{geom}	*Number of transitions*
n-Hexane, CH_2—CH_2	K_{φ_n}	δ_n	m_n	$CS_{12}(CH_2, CH_2)$	$CS_6(CH_2, CH_2)$	*[kJ/mol]*	*[atm]*	[%]	*[per dihedral per 100 ps]*
Experimental target						**31.55**	**0.20**	**65(66)**	–
GROMOS96 43A1	5.86	+1	3	0.7112889E-05	0.4723813E-02	31.87	31.12	86, 80, 86	2.33, 3.38, 2.37
GROMOS96a	7.08	+1	3	0.4741926E-05	0.4723813E-02	31.80	−3.72	67, 71, 67	2.36, 1.94, 2.30
GROMOS96b	6.28	+1	3	0.4459842E-05	0.4723813E-02	31.78	9.35	65, 68, 65	3.64, 3.05, 3.59
GROMOS96c 43A2	5.92	+1	3	0.4741926E-05	0.4723813E-02	31.63	0.44	63, 71, 63	4.39, 3.60, 4.39
GROMOS96d	6.28	+1	3	0.4459842E-05	0.4723813E-02	31.70	2.10	63, 69, 63	3.58, 3.06, 3.56
OPLS ua	2.95181	+1	1	0.0	0.0	32.07	4.08	70, 77, 70	3.05, 2.55, 3.07
	−0.56693	−1	2						
	6.57934	+1	3						
OPLS aa	3.640080	+1	1	0.1866303E-05	0.1015252E-02	32.07	166.02	80, 84, 80	1.51, 1.27, 1.41
	−0.328444	−1	2						
	0.583668	+1	3						

The trajectories of configurations were used after 100 ps of equilibration time to calculate the average energy, the average pressure, the geometric *trans-gauche* ratio (Eq. (4)), and the number of transitions of dihedral angles, from which both the frequency of transition and the transition-derived *trans-gauche* ratio (Eq. (5)) can be calculated. The geometric definition of the percentage of *trans* conformations depends on the number of *trans* configurations n_{φ_t} and the number of *gauche* configurations n_{φ_g} in the trajectory:

$$\langle r_{\text{geom}} \rangle = \frac{\sum n_{\varphi_t} \cdot 100}{\sum n_{\varphi_t} + \sum n_{\varphi_g}}, \quad \text{for} \begin{array}{l} \varphi = \{-180° \cdots +180°\} \\ \varphi_t = |\varphi| > 120° \\ \varphi_g = |\varphi| < 120° \end{array} \tag{4}$$

The geometric *trans-gauche* ratio is obtained by defining the top of the *trans-gauche* torsional energy barrier ($\varphi = \pm 120°$) as the separation line. In the same vein, one could define a dihedral angle transition to occur if the dihedral angle passes this barrier. However, if the dihedral angle immediately returns backwards over the barrier, one would not consider such crossing events as two transitions. Therefore, for the dihedral transitions, the definition used in the GROMOS package was applied [11]. A dihedral transition is only considered to be completed if the dihedral angle passes the bottom of an adjacent well in the dihedral energy term (1). Then the time difference Δt_{φ_t} between two subsequent transitions from and to the *trans* configuration and the corresponding time difference Δt_{φ_g} can be used to define a transition-derived percentage of *trans* conformations:

$$\langle r_{\text{trans}} \rangle = \frac{\sum \Delta t_{\varphi_t} \cdot 100}{\sum \Delta t_{\varphi_t} + \sum \Delta t_{\varphi_g}}, \quad \begin{array}{l} \Delta t_{\varphi_t} = t_{\varphi_t} \rightarrow t_{\varphi_g} \\ \Delta t_{\varphi_g} = t_{\varphi_g} \rightarrow t_{\varphi_t} \end{array} \tag{5}$$

Time differences in Eq. (5) have been taken from the registered transitions of the dihedral angles of the same type. In all cases, the transition-derived average *trans-gauche* ratios are within 10% of the average geometrical *trans-gauche* ratios. For the parametrisation, only the geometrical *trans-gauche* ratios have been taken into account and only this data is shown in Table II.

To calculate the heat of vaporization simulations in vacuum are required. The final coordinates and velocity vectors of the liquid simulation trajectory have been used to initialise simulations in vacuum. The 512 molecules were redistributed into a much larger box of 400 nm side length to avoid intermolecular interactions. With this large cubic box and a single cutoff of 1.0 nm, a vacuum trajectory of 100 ps was produced (50 ps equilibration time). From the potential energies E_{pot} of the liquid and

Downloaded At: 18:55 14 January 2011

vacuum simulations the heat of vaporization for the pure substance was calculated using Eq. (6) which simply corresponds to the enthalpy difference $H_{gas} - H_{liquid}$. The average total potential molecular energy of the liquid phase is subtracted from the average total potential molecular energy lacking the intermolecular contacts in the gas phase under the assumption of ideality in the gas using RT replacing pV,

$$\Delta H_{vap} = E_{pot}(g) - E_{pot}(l) + RT. \tag{6}$$

4. RESULTS AND DISCUSSION

The van der Waals repulsive parameter CS_{12} of the GROMOS96 43A1 force field shows a too large repulsion between third neighbours in the energy as function of dihedral angle for aliphatic chains. *n*-Butane shows the largest deviation in energy levels using the original GROMOS96 parameters.

As can be seen in Table II, the simulated percentage of *trans* conformers is too large, 91, 86 and (86, 80, 86) percent for the three *n*-alkane liquids as compared to the target values of 60, 64 and 65 percent, respectively. The *trans-gauche* ratio can be reduced by decreasing the third-neighbour repulsive van der Waals parameters CS_{12}. This decrease will also reduce the *trans/gauche* energy barriers which can be counteracted by increasing the force constant of the torsional angle energy term K_{φ_n}. These parameter changes will also affect the heat of vaporization and the pressure of the liquids. A large number of parameter value combinations was tested. The results for a few of these are shown in Table II. The amplitude of the dihedral potential energy term was either set to fit the barrier height of *n*-hexane (models b, c and d) or *n*-butane (model a). This affects the kinetics of dihedral transitions and in the case of *n*-hexane changed the molecular kinetics completely: the central dihedral is less mobile than the end dihedral angles. Large deviations in the heat of vaporization were not observed using the new models a to d, but the sampling of dihedral space is indeed different compared to GROMOS96 43A1 and also the pressure was positively affected. The modification indicated by the symbol GROMOS96c yields the best agreement with the nine target values. Compared to the GROMOS96 43A1 results these parameters yield a significant improvement of the *trans-gauche* ratio, while agreeing even slightly better with the target values for the heat of vaporization and pressure.

Table II also contains values for the OPLS united-atom [12, 47] and all-atom [13, 46, 48] force fields. The OPLS united-atom parameters which are

Downloaded At: 18:55 14 January 2011

relatively old, yield surprisingly good agreement with the target values, which were partially not yet available in 1984. The much newer OPLS all-atom model produces too high pressures and too large *trans-gauche* ratios.

The OPLS parameters originate from (N, P, T) Monte Carlo simulations using a 1.1 nm intermolecular non-bonded cut-off in the all-atom case [46] and values in the range of 0.95 to 1.5 nm in the united-atom case [47]. When fitting the OPLS force field parameters, a correction was made that approximately accounts for the non-bonded interactions between atom pairs at a distance larger than the cut-off distance (R_c). We have analysed the size of these long-range contributions to the energy and pressure as a function of cut-off radius in the appendix. The results for the three *n*-alkanes using GROMOS96 and OPLS force fields with a cut-off radius of 1.4 nm are shown in Table III. The contribution of forces beyond $R_c = 1.4$ nm enlarges the heat of vaporization by at most 1 kJ mol^{-1} and reduces the pressure by maximally 150 atm. Inclusion of the long-range contribution improves the agreement with experiment for *n*-butane, while for *n*-pentane and *n*-hexane the heat of vaporization becomes too large. For the latter

Downloaded At: 18:55 14 January 2011

TABLE III 1.4 nm cut-off contribution correction to heat of vaporization and pressure for *n*-alkanes. Heat of vaporization and pressure from MD simulations using a non-bonded cut-off radius $R_c = 1.4$ nm and the corresponding contributions E_{R_c} and p_{R_c} calculated using Eqs. (A.8) and (A.9). All simulation results have been obtained with the GROMOS96 program [11]. For further explanation see captions of Tables II, IV–VI and the methods section

	n-Butane		*n-Pentane*		*n-Hexane*	
	ΔH_{vap} kJ mol^{-1}	p atm	ΔH_{vap} kJ mol^{-1}	p atm	ΔH_{vap} kJ mol^{-1}	p atm
Experiment	21.62	2.4	26.43	0.68	31.55	0.20
GROMOS96 (43A1)						
MD	20.76	130	26.30	41	31.87	31
$-E_{R_c}$, p_{R_c}	0.61	−119	0.81	−137	1.01	−153
sum	21.37	11	27.11	−96	32.88	−122
GROMOS96 (43A2)						
MD	21.00	122	26.09	25	31.63	0
$-E_{R_c}$, p_{R_c}	0.61	−119	0.81	−137	1.01	−153
sum	21.61	3	26.90	−112	32.64	−153
OPLS-UA						
MD	21.05	130	26.25	40	32.07	4
$-E_{R_c}$, p_{R_c}	0.62	−121	0.82	−139	1.02	−154
sum	21.67	9	27.07	−99	33.09	−150
OPLS-AA						
MD	21.20	131	26.37	118	32.07	166
$-E_{R_c}$, p_{R_c}	0.38	−75	0.51	−86	0.64	−96
sum	21.58	56	26.88	32	32.71	70

two liquids the pressure becomes too low for the united-atom models and it is still a bit too high for the OPLS all-atom model.

We note that the evaluation of the long-range contributions from pairs beyond the cut-off distance using Eqs. (A.8 – 9) is only possible for systems with an isotropic and homogeneous distribution in space of the different types of atom pairs, such as pure liquids or simple mixtures. For proteins and DNA in aqueous solution or membranes, such contributions cannot be estimated using (A.8 – 9), but should be explicitly calculated. The GROMOS96 force field has therefore been parametrised using a relatively long cut-off of 1.4 nm and without any corrections of the type of Eqs. (A.8 – 9). This 1.4 nm cut-off radius is thus a parameter of the GROMOS96 force field. When comparing results in Table III, the pure MD-simulation results should be used for GROMOS96, whereas the long-range contributions $-E_{R_c}$ and p_{R_c} should be included for OPLS. For *n*-butane the OPLS results agree better than the GROMOS96 ones with experiment, whereas for *n*-pentane and *n*-hexane the GROMOS96 results are better than both OPLS united-atom and all-atom results. This illustrates the observation that a more complex model need not necessarily give better results than a simple model. One should note that for proteins an all-atom model almost quadruples the number of non-bonded interactions to be calculated compared to a united-atom model. For membrane simulations the computational effort will be increased by an even larger factor.

Downloaded At: 18:55 14 January 2011

5. CONCLUSIONS

The dihedral angle energy parameter K_{φ_n} for dihedral angles of type $\square—CH_n—CH_n—\square$ and the third-neighbour van der Waals repulsive parameters for atom types CH_2 and CH_3 of the GROMOS 43A1 set of force field parameters have been modified to better fit the heat of vaporization, pressure and *trans-gauche* ratio for liquid *n*-butane, *n*-pentane and *n*-hexane. The new parameter set, denoted GROMOS 43A2 yields significantly better results than the 43A1 set.

When comparing the mentioned properties calculated using OPLS united-atom force field parameters and OPLS all-atom force field parameters with the GROMOS 43A2 parameters, the OPLS force fields perform better for *n*-butane, whereas the GROMOS96 force field does better for *n*-pentane and *n*-hexane. This illustrates that a more complex and time consuming (all-atom) model need not necessarily yield better results than

a simple (united-atom) one. This finding suggests that the efficiency of biomolecular simulation will benefit from the use and development of united-atom models.

Acknowledgements

We would like to thank Pier L. Luisi for this scientific collaboration and financial support, Alexandre Bonvin, Wolfgang Damm, Xavier Daura and Alan Mark for their help and advice, and Peter Walde for stimulating discussions.

APPENDIX

Energy and Pressure Corrections for Finite Cut-off

The use of a cut-off radius (R_c) for non-bonded interactions in a molecular simulation is only allowed if the contribution of the forces between atoms at a distance larger than R_c is negligible, or if a good approximation of these forces can be formulated. For a homogeneous atomic liquid the contribution of atom pairs at a distance beyond R_c to the potential energy is [49].

$$E_{R_c} = 2\pi N_{\text{at}}^2 V^{-1} \int_{R_c}^{\infty} r^2 V^{\text{nonb}}(r) g(r) dr, \tag{A.1}$$

and to the pressure it is

$$p_{R_c} = -\frac{1}{3} 2\pi N_{\text{at}}^2 V^{-2} \int_{R_c}^{\infty} r^2 \left(r \frac{dV^{\text{nonb}}}{dr} \right) g(r) dr. \tag{A.2}$$

The number of atoms in the volume V is N_{at}, $V^{\text{nonb}}(r)$ is the non-bonded atom–atom interaction, and $g(r)$ is the atom–atom radial distribution function. The integrals in (A.1) and (A.2) can be calculated when $V^{\text{nonb}}(r)$ and $g(r)$ are known. For a non-bonded interaction of Lennard-Jones type,

$$V^{\text{nonb}}(r) = \frac{C_{12}}{r^{12}} - \frac{C_6}{r^6} \tag{A.3}$$

and for large values of R_c one may use the approximations

$$V^{\text{nonb}}(r) = -C_6 r^{-6} \tag{A.4}$$

Downloaded At: 18:55 14 January 2011

and

$$g(r) = 1. \tag{A.5}$$

Then one obtains for a system of N_{at} atoms

$$E_{R_c} = -\frac{2\pi}{3}\frac{N_{at}^2}{V}\frac{C_6}{R_c^3} \tag{A.6}$$

and

$$p_{R_c} = -\frac{4\pi}{3}\left(\frac{N_{at}}{V}\right)^2\frac{C_6}{R_c^3} = 2E_{R_c}V^{-1}. \tag{A.7}$$

For a system of $N_{molecule}$ molecules, each consisting of N_{am} atoms per molecule, the value of E_{R_c} *per molecule* is

$$E_{R_c}^{mol} = -\frac{2\pi}{3}\frac{N_{at}}{V}\frac{C_6}{R_c^3}N_{am} \tag{A.8}$$

and

$$p_{R_c} = 2E_{R_c}^{mol}V^{-1}N_{molecule}. \tag{A.9}$$

The expressions $E_{R_c}^{mol}$ and p_{R_c} were evaluated for the homogeneous systems of *n*-butane, *n*-pentane and *n*-hexane using cut-off radii R_c ranging from 0.8 to 1.8 nm and C_6 parameters from the GROMOS96 and OPLS force fields. The C_6 parameters are listed in Table IV. Since the *n*-alkanes contain two types of atoms, CH_2 and CH_3 in the united-atom representation,

TABLE IV Lennard-Jones C_6 attractive parameters for intermolecular non-bonded interactions. Attractive intermolecular non-bonded interaction parameters C_6 (see Eq. (2)), in kJ mol^{-1} nm^6, for alkanes or aliphatic chains in the GROMOS96 (43A1, 43A2) [11], OPLS united atom (UA) [47] and OPLS all-atom (AA) [46] force fields

Pairtype	*Force field GROMOS96*	*Force field OPLS-UA*	*Pair type*	*Force field OPLS-AA*
CH_2—CH_2	0.007105	0.007003	C—C	0.00203050
CH_2—CH_3	0.008394	0.008528	C—H	0.00049889
CH_3—CH_3	0.009916	0.010385	H—H	0.00012258

Downloaded At: 18:55 14 January 2011

and C and H in the all-atom representation, the C_6 value used in Eqs. (A.8 – 9) is a weighted sum of the C_6 values of each type of atom pair with the fraction of each pair type given in Table V as weight factor. Table VI contains the heat of vaporization and pressure as obtained from MD simulations, and the values of expressions (A.8) and (A.9) for different cut-off radii R_c. Beyond $R_c = 1.4$ nm the long-range contributions become rather small compared to other approximations inherent to the force fields. Below $R_c = 1.0$ nm, the assumptions of homogeneity (generally a charge-group or molecular cut-off is used in biomolecular force fields), and Eq. (A.5) become incorrect, especially for the larger *n*-hexane.

The OPLS parameters have been obtained by fitting of the heat of vaporization and the density of *n*-alkanes in (N, P, T) Monte Carlo simulations of the liquids [46, 47]. It is explicitly stated in [46, 47] that the contribution E_{R_c} to the energy was included in the fitting of the heat of vaporization. However, nothing is stated in [46, 47] about inclusion of the corresponding contribution p_{R_c} to the pressure when fitting to the experimental density.

When deriving the force field parameters of the GROMOS96 force field, the contributions E_{R_c} and p_{R_c} were not considered [14], since a relatively long cut-off radius $R_c = 1.4$ nm was used for both the electrostatic and van der Waals interactions, which makes these contributions rather small.

Downloaded At: 18:55 14 January 2011

TABLE V Densities of molecules, atoms and pairs of atoms of different types. For further explanation see text of methods section and the appendix

	n-Butane	*n-Pentane*	*n-Hexane*
Box volume [nm^3]	86.2419	98.7803	110.9620
Number of molecules in box [N_{molecule}]	512	512	512
Number of atoms			
per molecule [N_{am}]:			
united-atom models (CH_2, CH_3)	4 (2, 2)	5 (3, 2)	6 (4, 2)
all-atom models (C, H)	14 (4, 10)	17 (5, 12)	20 (6, 14)
in box [N_{at}]:			
united-atom models	2048	2560	3072
all-atom models	7168	8704	10240
Fraction of atom pairs of types			
for united-atom models:			
CH_2—CH_2	4/16	9/25	16/36
CH_2—CH_3	8/16	12/25	16/36
CH_3—CH_3	4/16	4/25	4/36
for all atom models:			
C—C	16/196	25/289	36/400
C—H	80/196	120/289	168/400
H—H	100/196	144/289	196/400

Downloaded At: 18:55 14 January 2011

TABLE VI Effect of the intermolecular non-bonded interaction cut-off radius R_c on the simulated heat of vaporization and pressure, and the corresponding contributions E_{R_c} and p_{R_c} calculated using Eqs. (A.8) and (A.9). For further explanation see captions of Tables II–V

		*GROMOS*96 (43*A*2)						*OPLS-UA*						*OPLS-AA*					
R_c[*nm*]	*exp.*	0.8	1.0	1.2	1.4	1.6	1.8	0.8	1.0	1.2	1.4	1.6	1.8	0.8	1.0	1.2	1.4	1.6	1.8
n-Butane																			
ΔH_{vap} [kJ mol^{-1}]																			
MD	–	17.43	19.38	20.26	21.00	20.92	21.05	17.76	19.85	20.66	21.05	21.29	21.48	20.52	21.09	21.25	21.20	21.27	21.15
$-E_{R_c}$	–	3.28	1.68	0.97	0.61	0.41	0.29	3.35	1.71	0.99	0.62	0.42	0.29	2.06	1.05	0.61	0.38	0.26	0.18
sum	21.62	20.71	21.06	21.23	21.61	21.33	21.34	21.11	21.56	21.65	21.67	21.71	21.77	22.58	22.14	21.86	21.58	21.53	21.33
p [atm]																			
MD	–	786	392	191	122	63	51	810	402	202	130	79	59	438	292	171	131	108	100
p_{R_c}	–	−639	−327	−189	−119	−80	−56	−651	−333	−193	−121	−81	−57	−400	−205	−119	−75	−50	−35
sum	2.43	147	65	2	3	−17	−5	159	69	9	9	−2	2	38	87	52	56	58	65
n-Pentane																			
ΔH_{vap} [kJ mol^{-1}]																			
MD	–	21.19	24.22	25.60	26.09	26.55	26.72	20.92	24.24	25.64	26.25	26.63	26.67	24.98	26.02	26.42	26.37	26.61	26.31
$-E_{R_c}$	–	4.33	2.22	1.28	0.81	0.54	0.38	4.39	2.25	1.30	0.82	0.55	0.39	2.72	1.39	0.81	0.51	0.34	0.24
sum	26.43	25.52	26.44	26.88	26.90	27.09	27.10	25.31	26.49	26.94	27.07	27.18	27.06	27.70	27.41	27.23	26.88	26.95	26.55
p [atm]																			
MD	–	969	380	147	25	−31	−42	966	382	147	40	−20	−38	506	275	175	118	74	53
p_{R_c}	–	−736	−377	−218	−137	−92	−64	−745	−382	−221	−139	−93	−65	−462	−237	−137	−86	−58	−41
sum	0.68	233	3	−71	−112	−123	−106	221	0	−74	−99	−113	−103	44	38	38	32	16	12
n-Hexane																			
ΔH_{vap} [kJ mol^{-1}]																			
MD	–		28.94	30.83	31.63	32.14	32.33		29.18	31.10	32.07	32.41	32.72		31.49	32.16	32.07	32.01	32.12
$-E_{R_c}$	–		2.78	1.61	1.01	0.68	0.48		2.80	1.62	1.02	0.68	0.48		1.75	1.01	0.64	0.43	0.30
sum	31.55		31.72	32.44	32.64	32.82	32.81		31.98	32.72	33.09	33.09	33.20		33.24	33.17	32.71	32.44	32.42
p [atm]																			
MD	–		452	158	0	−56	−116		466	140	4	−55	−100		313	228	166	134	134
p_{R_c}	–		−420	−243	−153	−103	−72		−424	−245	−154	−103	−73		−264	−153	−96	−65	−45
sum	0.20		32	−85	−153	−159	−188		42	−105	−150	−158	−173		49	75	70	69	89

References

[1] Levitt, M. (1974). "Energy refinement of hen-egg white lysozyme", *J. Mol. Biol.*, **82**, 393.

[2] Levitt, M., Hirshberg, M., Sharon, R. and Daggett, V. (1995). "Potential energy function and parameters for simulations of the molecular dynamics of proteins and nucleic acids in solution", *Comp. Phys. Com.*, **91**, 215.

[3] Hagler, A. T., Huler, E. and Lifson, S. (1974). "Energy functions for peptides and proteins. 1. Derivation of a consistent force field including the hydrogen bond from amide crystals", *J. Am. Chem. Soc.*, **96**, 5319.

[4] Dauber-Osguthorpe, P., Roberts, V. A., Osguthorpe, D. J., Wolff, J., Genest, M. and Hagler, A. T. (1988). "Structure and energetics of ligand binding to proteins: E. coli dihydrofolate reductase-trimethoprim, a drug-receptor system", *PROTEINS: Structure, Function and Genetics*, **4**, 31.

[5] Brooks, B. R., Bruccoleri, R. E., Olafson, B. D., States, D. J., Swaminathan, S. and Karplus, M. (1983). "CHARMM: A program for macromolecular energy minimization and dynamics calculations", *J. Comp. Chem.*, **4**, 187.

[6] MacKerell, Jr., Bashford, A. D., Bellott, M., Dunbrack, Jr., Evanseck, J. D., Field, M. J., Fischer, S., Gao, J., Guo, H., Ha, S., Joseph-McCarthy, D., Kuchnir, L., Kuczera, K., Lau, F. T. K., Mattos, C., Micknick, S., Ngo, T., Nguyen, D. T., Prodhom, B., Reiher III, W. E., Roux, B., Schlenkrich, M., Smith, J. C., Stote, R., Straub, J., Watanabe, M., Wiorkiewicz-Kuczera, J., Yin, D. and Karplus, M. (1998). "All-atom empirical potential for molecular modeling and dynamics studies of proteins", *J. Phys. Chem. B*, **102**, 3586.

[7] Weiner, S. J., Kollman, P. A., Case, D. A., Singh, U. C., Ghio, C., Alagona, G., Profeta, S. Jr. and Weiner, P. (1984). "A new force field for molecular mechanical simulation of nucleic acids and proteins", *J. Am. Chem. Soc.*, **106**, 765.

[8] Cornell, W. D., Cieplak, P., Bayly, C. I., Gould, I. R., Merz, K. M. Jr., Ferguson, D. M., Spellmeyer, D. C., Fox, T., Caldwell, J. W. and Kollman, P. A. (1995). "A second generation force field for the simulation of proteins, nucleic acids and organic molecules", *J. Am. Chem. Soc.*, **117**, 5179.

[9] Hermans, J., Berendsen, H. J. C., van Gunsteren, W. F. and Postma, J. P. M. (1984). "A consistent empirical potential for water-protein interactions", *Biopolymers*, **23**, 1513.

[10] Egberts, E., Marrink, S. J. and Berendsen, H. J. C. (1994). "Molecular dynamics simulation of a phospholipid membrane", *Eur. Biophys. J.*, **22**, 423.

[11] van Gunsteren, W. F., Billeter, S. R., Eising, A. A., Hünenberger, P. H., Krüger, P., Mark, A. E., Scott, W. R. P. and Tironi, I. G., "Biomolecular Simulation, The GROMOS96 Manual and User Guide", *vdf Hochschulverlag AG an der ETH Zürich and BIOMOS b.v.*, Zürich, Groningen, 1996.

[12] Jorgensen, W. L. and Tirado-Rives, J. (1988). "The OPLS potential functions for proteins. Energy minimization for crystals of cyclic peptides and crambin", *J. Am. Chem. Soc.*, **110**, 1657.

[13] Jorgensen, W. L., Maxwell, D. S. and Tirado-Rives, J. (1996). "Development and testing of the OPLS all-atom force field on conformational energetics and properties of organic liquids", *J. Am. Chem. Soc.*, **118**, 11225.

[14] Daura, X., Mark, A. E. and van Gunsteren, W. F. (1998). "Parametrization of aliphatic CH_n united atoms of GROMOS96 force field", *J. Comp. Chem.*, **19**, 535.

[15] van Gunsteren, W. F., Daura, X. and Mark, A. E. (1998). "The GROMOS force field", *Encyclopaedia of Comp. Chem.*, **2**, 1211.

[16] van Gunsteren, W. F. and Berendsen, H. J. C., "Groningen Molecular Simulation (GROMOS), Library Manual", *BIOMOS b.v.*, Groningen, 1987.

[17] "*TRC Thermodynamic Tables-Hydrocarbons*", Texas A&M University System, College Station, TX.

[18] Sasz, G. J., Sheppard, N. and Rank, D. H. (1948). "Spectroscopic studies of rotational isomerism. I. Liquid butane and the assignement of the normal modes of vibration", *J. Chem. Phys.*, **16**, 704.

[19] Sheppard, N. and Sasz, G. J. (1949). "Spectroscopic studies of rotational isomerism. III. The normal paraffins in the liquid and solid states", *J. Chem. Phys.*, **17**, 86.

[20] Flory, P. J., "*Statistical mechanics of chain molecules*", Wiley-Interscience: New York, 1969.

Downloaded At: 18:55 14 January 2011

[21] Verma, A. L., Murphy, W. F. and Bernstein, H. J. (1974). "Rotational isomerism. XI. Raman spectra of butane, 2-methylbutane and 2,3-dimethylbutane", *J. Chem. Phys.*, **60**, 1540.
[22] Bradford, W. F., Fitzwater, S. and Bartell, L. S. (1977). "Molecular structure of *n*-butane: calculation of vibrational shrinkages and an electron diffraction reinvestigation", *J. Mol. Struct.*, **38**, 185.
[23] Durig, J. R. and Compton, D. A. C. (1979). "Analysis of torsional spectra of molecules with two internal C_{3v} Rotors. $12^{[a]}$. Low frequency vibrational spectra, methyl torsional function, and internal rotation of *n*-butane", *J. Phys. Chem.*, **83**, 265.
[24] Colombo, L. and Zerbi, G. (1980). "Enthalpy difference of rotational isomers in liquid butane and pentane from infrared spectra", *J. Chem. Phys.*, **73**, 2013.
[25] Kint, S., Scherer, J. R. and Snyder, R. G. (1980). "Raman spectra of liquid *n*-alkanes. III. Energy difference between *trans* and *gauche* *n*-butane", *J. Chem. Phys.*, **73**, 2599.
[26] Compton, D. A. C., Montero, S. and Murphy, W. F. (1980). "Low-frequency Raman spectrum and asymmetric potential function for internal rotation of gaseous *n*-butane", *J. Chem. Phys.*, **84**, 3587.
[27] Räsänen, M. and Bondybey, V. E. (1985). "Rotamerization of normal-butane in solid neon example of a mode specific chemical-reaction", *J. Chem. Phys.*, **82**, 4718.
[28] Hüttner, W., Majer, W. and Kästle, H. (1989). "Ground-state rotational spectrum and spectroscopic parameters of the *gauche* butane conformer", *Mol. Phys.*, **67**, 131.
[29] Snyder, R. G. and Kim, Y. (1991). "Conformation and low-frequency isotropic Raman-spectra of the liquid *n*-alkanes C4–C9", *J. Phys. Chem.*, **95**, 602.
[30] Durig, J. R., Wang, A., Beshir, W. and Little, T. S. (1991). "Barrier to asymmetric internal rotation, conformational stability, vibrational spectra and assignments, and *ab initio* calculations of *n*-butane-d_0, d_5 and d_{10}", *J. Raman Spectrosc.*, **11**, 683.
[31] Murphy, W. F., Fernandez-Sanchez, J. M. and Raghavachari, K. (1991). "Harmonic force-field and Raman-scattering intensity parameters of normal-butane", *J. Phys. Chem.*, **95**, 1124.
[32] Frey, R. F., Cao, M., Newton, S. Q. and Schäfer, L. (1993). "Electron correlation-effects in aliphatic nonbonded interactions comparison of *n*-alkane MP2 and HF geometries", *J. Mol. Struct. (Theochem)*, **285**, 99.
[33] Herrebout, W. A., van der Veken, B., Wang, A. and Durig, J. R. (1995). "Enthalpy difference between conformers of *n*-butane and the potential function governing conformational interchange", *J. Phys. Chem.*, **99**, 578.
[34] Maxwell, D. S., Tirado-Rives, J. and Jorgensen, W. L. (1995). "A comprehensive study of the rotational energy profiles of organic-systems by *ab-initio* MO theory, forming a basis for peptide torsional parameters", *J. Comp. Chem.*, **16**, 984.
[35] Smith, G. D. and Jaffe, R. L. (1996). "Quantum chemistry study of conformational energies and rotational energy barriers of *n*-alkanes", *J. Phys. Chem.*, **100**, 18718.
[36] Allinger, N. L., Fermann, J. T., Allen, W. D. and Schaefer III, H. F. (1997). "The torsional conformations of butane: definitive energetics from *ab initio* methods", *J. Chem. Phys.*, **106**, 5143.
[37] Mizushima, S. and Okazaki, H. (1949). "Equilibrium ratio of rotational isomers of *n*-pentane: with special reference to its difference from that of 1,2-dichloroethane", *J. Am. Chem. Soc.*, **71**, 3411.
[38] Harada, I., Takeuchi, H., Sakakibara, M., Matsuura, H. and Shimanouchi, T. (1977). "Vibration spectra and rotational isomerism of chain molecules. II. Butane, pentane, hexane, pentane-d_{12}, and hexane-d_{14}", *Bull. Chem. Soc. Jpn.*, **50**, 102.
[39] Maissara, M., Cornut, J. C., Devaure, J. and Lascombe, J. (1983). "Conformational equilibrium of pentane as a function of temperature and pressure", *Spectrosc. Int. J.*, **2**, 104.
[40] Kanesaka, I., Snyder, R. G. and Strauss, H. L. (1986). "Experimental-determination of the *trans-gauche* energy difference of gaseous *n*-pentane and diethylether", *J. Chem. Phys.*, **84**, 395.
[41] Scherer, J. R. and Snyder, R. G. (1980). "Raman spectra of liquid *n*-alkanes. II. Longitudinal acoustic modes and the *gauche-trans* energy difference", *J. Phys. Chem.*, **72**, 5798.

Downloaded At: 18:55 14 January 2011

[42] Scott, W. R. P., Hünenberger, P. H., Tironi, I. G., Mark, A. E., Billeter, S. R., Fennen, J., Torda, A. E., Huber, T., Krüger, P. and van Gunsteren, W. F. (1999). "The GROMOS biomolecular simulation program package", *J. Phys. Chem. A*, **103**, 3596.
[43] Bonham, R. A. and Bartell, L. S. (1959). "The molecular structure and rotational isomerisation of *n*-butane", *J. Am. Chem. Soc.*, **81**, 3491.
[44] Berendsen, H. J. C., Postma, J. P. M., van Gunsteren, W. F., DiNola, A. and Haak, J. R. (1984). "Molecular dynamics with coupling to an external bath", *J. Chem. Phys.*, **81**, 3684.
[45] Ryckaert, J. P., Ciccotti, G. and Berendsen, H. J. C. (1977). "Numerical integration of the cartesian equations of motion of a system with constraints: Molecular dynamics of *n*-alkanes", *J. Comput. Phys.*, **23**, 327.
[46] Kaminski, G., Duffy, E. M., Matsui, T. and Jorgensen, W. L. (1994). "Free energies of hydration and pure liquid properties of hydrocarbons from the OPLS all-atom model", *J. Phys. Chem.*, **98**, 13077.
[47] Jorgensen, W. L., Madura, J. D. and Swenson, C. J. (1984). "Optimized intermolecular potential functions for liquid hydrocarbons", *J. Am. Chem. Soc.*, **106**, 6638.
[48] Jorgensen, W. L., "BOSS", Version 4.0, Yale University: New Haven, CT, 1998.
[49] Allen, M. P. and Tildesley, D. J., "Computer simulation of liquids", Oxford University Press: New York, 1987.
[50] Chandrasekhar, I., "Parameter development for molecular dynamics simulation of lipids", in Biomembrane Structure & Function – The State of the Art, Adenine Press, Albany, NY, 1992.

Downloaded At: 18:55 14 January 2011